nature chemistry

Article

https://doi.org/10.1038/s41557-023-01345-4

Heteromultivalency enables enhanced detection of nucleic acid mutations

In the format provided by the authors and unedited

Table of Contents

Materials

Oligonucleotide Sequences and Modifications

All oligonucleotides were custom synthesized by Integrated DNA Technologies (Coralville, IA). The table below includes the names and sequences for all oligonucleotides used in this work. The structures of each of the oligonucleotide modifications are also included below.

Name	Sequence (5' to 3')
7S	/5ThioMC6-D/TTTTTTTTTTACAAGCT
8S	/5ThioMC6-D/TTTTTTTTTTCACAAGCT
9S	/5ThioMC6-D/TTTTTTTTTTCCACAAGCT
10S	/5ThioMC6-D/TTTTTTTTTTGCCACAAGCT
11S	/5ThioMC6-D/TTTTTTTTTTCGCCACAAGCT
4T	/5ThioMC6-D/TTTTTTTTTTCCAA
5T	/5ThioMC6-D/TTTTTTTTTTCCAAC
6T	/5ThioMC6-D/TTTTTTTTTTCCAACT
7T	/5ThioMC6-D/TTTTTTTTTTCCAACTA
8T	/5ThioMC6-D/TTTTTTTTTTCCAACTAC
9T	/5ThioMC6-D/TTTTTTTTTTCCAACTACC
10T	/5ThioMC6-D/TTTTTTTTTTCCAACTACCA
no spacer G12C	TGGTAGTTGGAGCTTGTGGCGTAGG/3AmMO/
no spacer WT	TGGTAGTTGGAGCTGGTGGCGTAGG/3AmMO/
internal short spacer G12C	TGGTAGTTGG/iSp9/AGCTTGTGGCGTAGG/3AmMO/
internal short spacer WT	TGGTAGTTGG/iSp9/AGCTGGTGGCGTAGG/3AmMO/
internal long spacer G12C	TGGTAGTTGG/iSp18/AGCTTGTGGCGTAGG/3AmMO/
internal long spacer WT	TGGTAGTTGG/iSp18/AGCTGGTGGCGTAGG/3AmMO/
terminal short spacer G12C	/5Sp9/TGGTAGTTGGAGCTTGTGGCGTAGG/3AmMO/
terminal short spacer WT	/5Sp9/TGGTAGTTGGAGCTGGTGGCGTAGG/3AmMO/
terminal long spacer G12C	/5Sp18/TGGTAGTTGGAGCTTGTGGCGTAGG/3AmMO/
terminal long spacer WT	/5Sp18/TGGTAGTTGGAGCTGGTGGCGTAGG/3AmMO/
3' thiol 8T	CCAACTACTTTTTTTTTT/3ThioMC3-D/
3' thiol 8S	CACAAGCTTTTTTTTTTT/3ThioMC3-D/
3' thiol 9S	CCACAAGCTTTTTTTTTTT/3ThioMC3-D/
5' thiol 8S L19F	/5ThioMC6-D/TTTTTTTTTTCGTGAAGG
5' thiol 9S L19F	/5ThioMC6-D/TTTTTTTTTTCGTGAAGGC
G12C/L19F	AGCTTGTGGCGTAGGCAAGAGTGCCTTCACG/3AmMO/
WT/L19F	AGCTGGTGGCGTAGGCAAGAGTGCCTTCACG/3AmMO/

G12C/WT	AGCTTGTGGCGTAGGCAAGAGTGCCTTGACG/3AmMO/
WT/WT	AGCTGGTGGCGTAGGCAAGAGTGCCTTGACG/3AmMO/
8S Q498R	GGTCGGAATTTTTTTTTT/3ThioMC3-D/
9S Q498R	GGGTCGGAATTTTTTTTTT/3ThioMC3-D/
8S Y505H	/5ThioMC6-D/TTTTTTTTTTGGTGACC
9S Y505H	/5ThioMC6-D/TTTTTTTTTTGGTGACCA
complement to 29 nt Omicron	/5ThioMC6D/TTTTTTTTTTGGTGACCAACACCATAAGTG GGTCGGAA
29 nt Omicron	TTCCGACCCACTTATGGTGTTGGTCACCA/3AmMO/
29 nt Original	TTCCAACCCACTAATGGTGTTGGTTACCA/3AmMO/
29 nt Alpha	TTCCAACCCACTTATGGTGTTGGTTACCA/3AmMO/
88 nt Omicron	/5AmMC6/AGGTTTTAATTGTTACTTTCCTTTACGATCATA TAGTTTCCGACCCACTTATGGTGTTGGTCACCAACCAT ACAGAGTAGTAGTACTT
88 nt Original	/5AmMC6/AGGTTTTAATTGTTACTTTCCTTTACAATCATA TGGTTTCCAACCCACTAATGGTGTTGGTTACCAACCAT ACAGAGTAGTAGTACTT
amine-modified forward primer	/5AmMC6/AGGTTTTAATTGTTACTTTCCTTTAC
reverse primer	AAGTACTACTACTCTGTATGGTTG

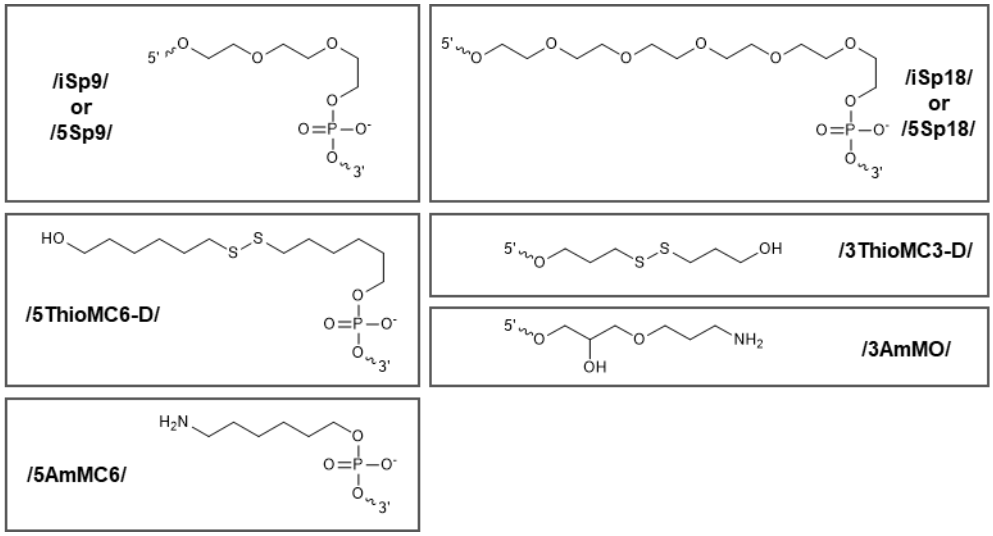

Reagents

5 µm aminated silica beads (Cat# SA06N) were purchased from Bangs Laboratory (Fishers, IN). Dri-solv methylsulfoxide (Cat# MX1457-7) was purchased from EMD Millipore (Burlington, MA). Potassium hydroxide (Cat# 221473), sodium bicarbonate (Cat#S6014), acetonitrile (Cat# 34998), and Atto647N NHS ester (Cat#18373-1MG-F) were purchased from Sigma-Aldrich (St. Louis, MO). 20x TE buffer (Cat# 42020325-2) was purchased from bioWORLD (Dublin, OH). Bond-Breaker TCEP (Tris(2-carboxyethyl)phosphine hydrochloride) solution, Neutral pH (Cat#77720), GeneAmp Fast PCR Master Mix (2x) (Cat# 4359187), High-Capacity cDNA Reverse Transcription kit (Cat# 4368814), Quant-IT Oligreen ssDNA reagent (Cat# O7582), SMCC (succinimidyl 4-(N-maleimidomethyl)cyclohexane-1-carboxylate) (Cat#22360), sulfo-NHS-acetate (Cat#26777), and Tween20 (Cat# BP337) were purchased from Thermo Fisher Scientific (Waltham, MA). Saline sodium citrate (SSC) buffer (Cat# AM9763) was purchased

from Ambion (Austin, TX). Triethylammonium acetate (Cat# 60-4110-57) was purchased from Glen Research (Sterling, VA). QIAamp Viral RNA mini kit (Cat# 52904) was purchased from Qiagen (Hilden, Germany). 30% Acrylamide/Bis Solution 29:1 (Cat# 1610156) was purchased from Bio-Rad (Hercules, CA). Heat-inactivated SARS-CoV-2 and human corona (229E, OC43) virus samples at known concentrations were provided by the NIH RADx-Radical Data Coordination Center (DCC) at the University of California San Diego and BEI Resources. Heat-inactivated SARS-CoV-2 Isolate hCoV-19/USA/CA-SEARCH-59467/2021 (Lineage BA.1; Omicron Variant) was contributed by Dr. Aaron Carlin and the UCSD CALM and EXCITE laboratories.

Consumables

96-well white flat bottom polystyrene microplates (Cat# 3912) were purchased from Corning (Corning, NY). P2 size exclusion gel (Cat#1504118) and P4 size exclusion gel (Cat# #1504124) was purchased from Bio-Rad (Hercules, CA). Nanosep MF centrifugal devices (Cat# ODM02C35) were purchased from Pall Laboratory.

Equipment

The major equipment that was used in this study includes: CytoFLEX V0-B3-R1 flow cytometer equipped with a 488 nm and 638 nm laser (Beckman coulter), Nanodrop 2000 UV-Vis Spectrophotometer (Thermo Scientific), Barnstead nanopure water purifying system (Thermo Fisher), 5424 R centrifuge (Eppendorf), Synergy H1 plate reader (Biotek), high-performance liquid chromatography 1100 (Agilent) with AdvanceBio Oligonucleotide C18 column (653950-702, 4.6x 150 mm, 2.7 µm) (Agilent), LTQ Orbitrap Velos mass spectrometer (Thermo Scientific), T100 thermal cycler (Bio-Rad), iBright FL1500 Imaging System (Thermo Fisher Scientific), Galaxy mini tabletop centrifuge (VWR), Rebel Brightfield Microscope (ECHO), and Nikon Ti2-E motorized research microscope equipped with SOLA SE II 365 Light Engine, Photometrics Prime 95B-25mm Back-illuminated sCMOS camera, and CF-L AT Cy5/Alexa 647/Draq 5 filter set.

Supplementary Figure 1. Description of targets and NUPACK predictions of target secondary structure.
(A) Scheme describing the DNA sequence (NCBI Reference Sequence: NG_007524.2) and amino acid sequence (NCBI Reference Sequence: NP_001356715.1) of the first 20 amino acids of human KRAS protein. The location of the no spacer targets used in this work are shown in red, with the G12C mutated codon shown in blue. (B and C) Predictions for the secondary structures of the no spacer G12C (B) and WT (C) targets generated using NUPACK. In the illustration on the left, the circle color of each nucleotide refers to the identity of each nucleobase. In the illustration on the right, the circle color of each nucleotide refers to the probability that each nucleotide is bound at equilibrium if it is shown bound or unbound if it is shown unbound. The black arrows refer to the position of the G12C mutation in the target sequence. (D) The location of the G12C/L19F targets used in this work are shown in red, with the G12C and L19F mutated codons shown in blue. (E, F, G, and H) Predictions for the secondary structures of the G12C/L19F (E), WT/L19F (F), G12C/WT (G), and WT/WT (H) targets generated using NUPACK. The black arrows refer to the position of the G12C and L19F mutations in the target sequence. (I) Scheme describing the DNA sequence (NCBI Reference Sequence: NC_045512.2) and amino acid sequence (NCBI Reference Sequence: YP_009724390.1) of amino acids 497-506 of SARS-CoV-2 spike protein. The location of the Omicron/Original/Alpha targets used in this work are shown in red, with the Q498R, N501Y, and Y505H mutated codons shown in blue. (J, K, L, M, and N) Predictions for the secondary structures of the 29 nt Omicron (J), 29 nt Original (K), 29 nt Alpha (L), 88 nt Original (M), and 88 nt Omicron (N) targets generated using NUPACK. The black arrows refer to the position of the Q498R, N501Y, and Y505 mutations in the target sequence. All predictions were performed at 0.15 M Na^{+}, 0 M Mg^{2+}, and 22°C.

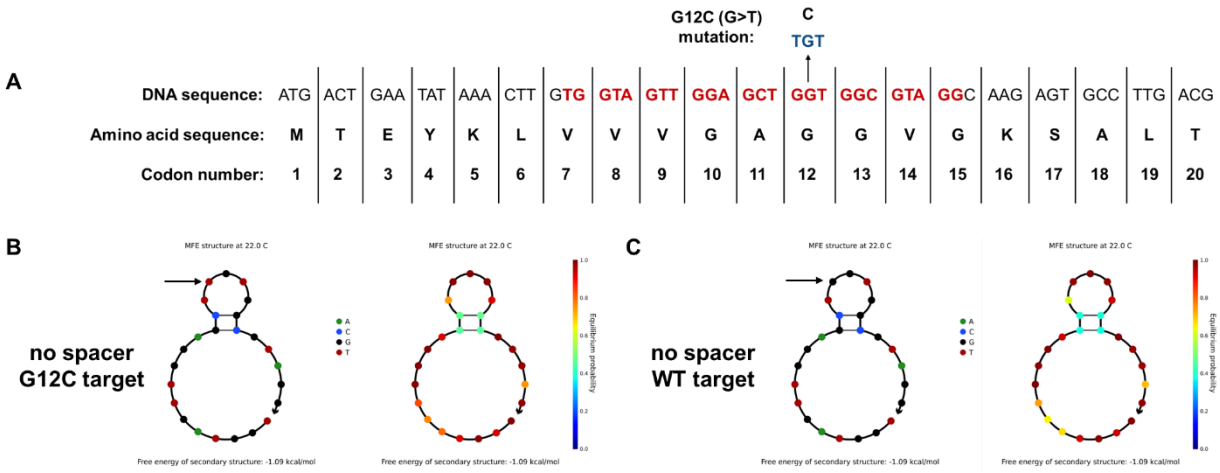
A
G12C (G>T) mutation:
C
TGT
DNA sequence: ATG ACT GAA TAT AAA CTT GTG GTA GTT GGA GCT GGT GGC GTA GGC AAG AGT GCC TTG ACG
Amino acid sequence: M T E Y K L V V V G A G G V G K S A L T
Codon number: 1 2 3 4 5 6 7 8 9 10 11 12 13 14 15 16 17 18 19 20
B
no spacer
G12C target
MFE structure at 22.0 C
A
C
G
T
Equilibrium probability
Free energy of secondary structure: -1.09 kcal/mol
C
no spacer
WT target

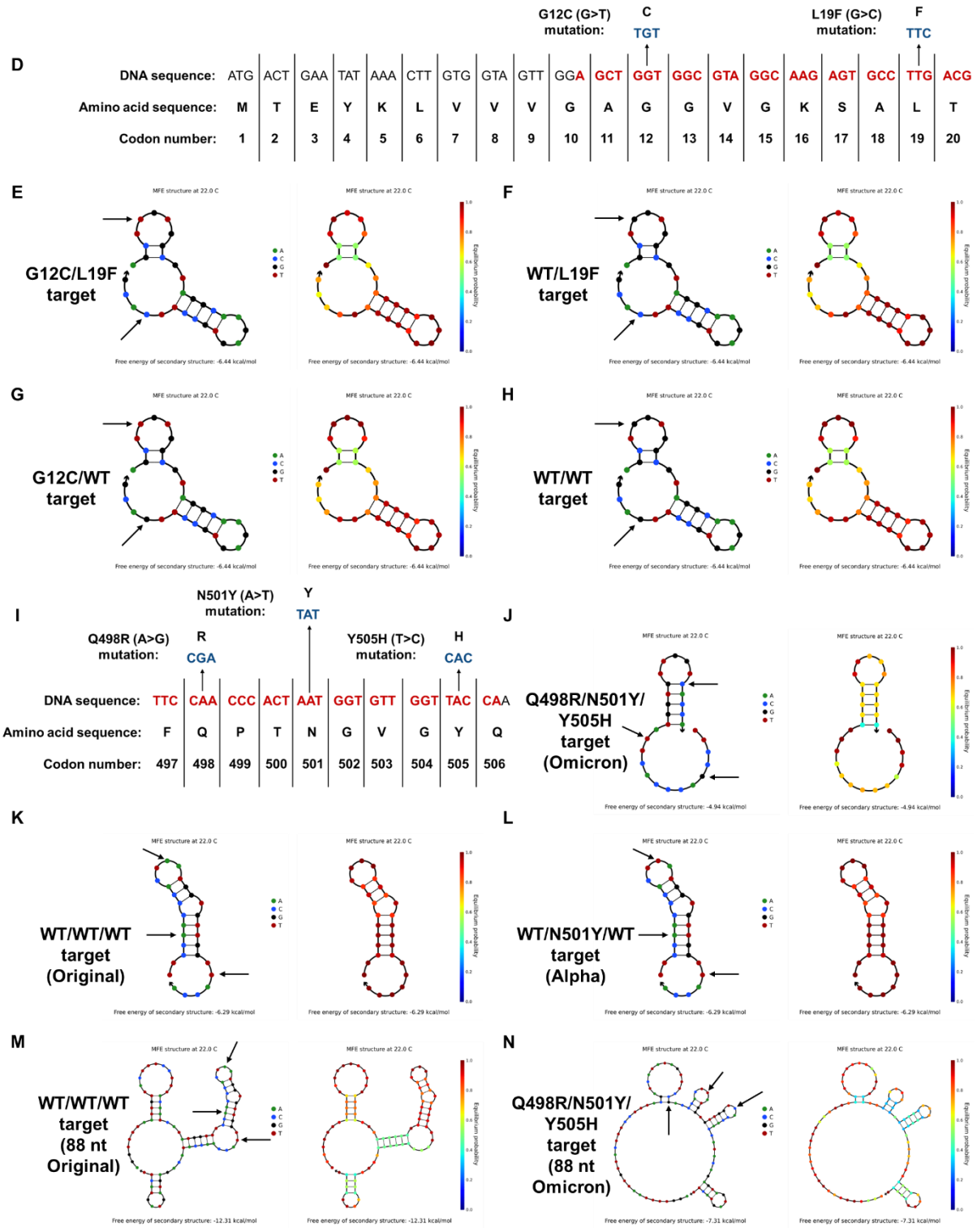

Supplementary Figure 2. Synthesis and purification of Atto647N-labeled targets.

(A) Reaction scheme for conjugation of 3’ amine-modified oligonucleotides with NHS-Atto647N. (B) HPLC traces of the 3’ Atto647N-labeled targets. (C) Reaction scheme for conjugation of 5’ amine-modified oligonucleotides with NHS-Atto647N. (D) HPLC traces of the 5’ Atto647N-labeled targets. Arrows represent the material collected from HPLC.

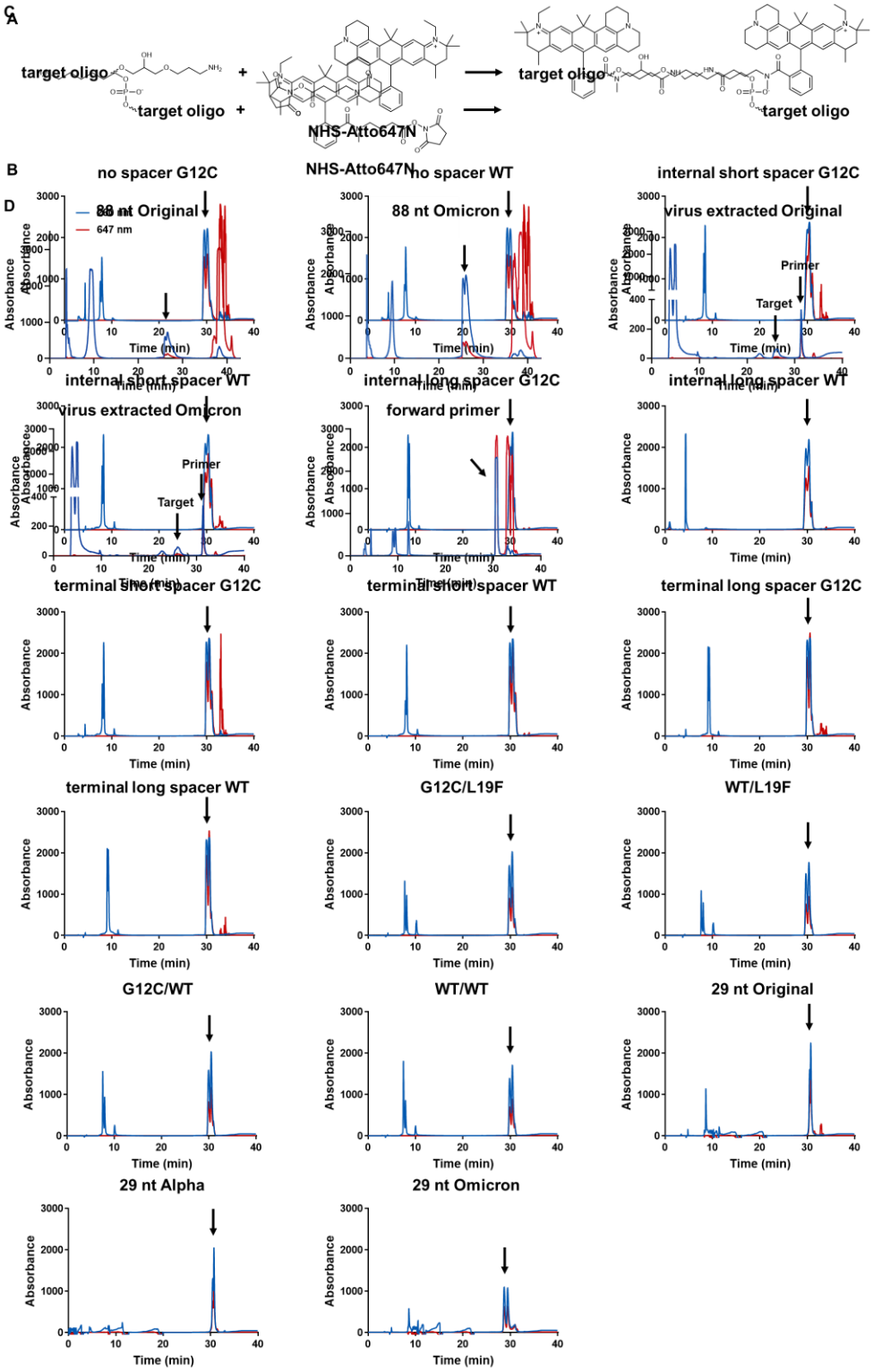

Supplementary Figure 3. Mass spectrometry characterization of Atto647N-labeled targets.

(A) Table of calculated masses, measured m/z values found, and difference in mass between calculated and measured masses of Atto647N-labeled targets. (B) Raw ESI mass spectra of Atto647N-labeled targets.

A

Sample	Calculated mass (Da)	m/z found (Da)	Difference (Da)
no spacer G12C	8680.17	8679.72	0.45
no spacer WT	8705.27	8704.72	0.55
internal short spacer G12C	8892.37	8891.76	0.61
internal short spacer WT	8917.37	8916.76	0.61
internal long spacer G12C	9024.47	9023.84	0.63
internal long spacer WT	9049.57	9048.84	0.73
terminal short spacer G12C	8892.37	8891.75	0.62
terminal short spacer WT	8917.37	8916.76	0.61
terminal long spacer G12C	9024.47	9023.83	0.64
terminal long spacer WT	9049.57	9048.84	0.73
G12C/L19F	10432.37	10431.01	1.36
WT/L19F	10457.37	10457.02	0.35
G12C/WT	10472.37	10472.02	0.35
WT/WT	10497.37	10497.03	0.34
29 nt Original	9667.87	9667.43	0.44
29 nt Alpha	9658.87	9658.41	0.46
29 nt Omicron	9659.87	9659.41	0.46
88 nt Original	27826.67	27827.96	-1.29
88 nt Omicron	27818.67	27817.95	0.72

B

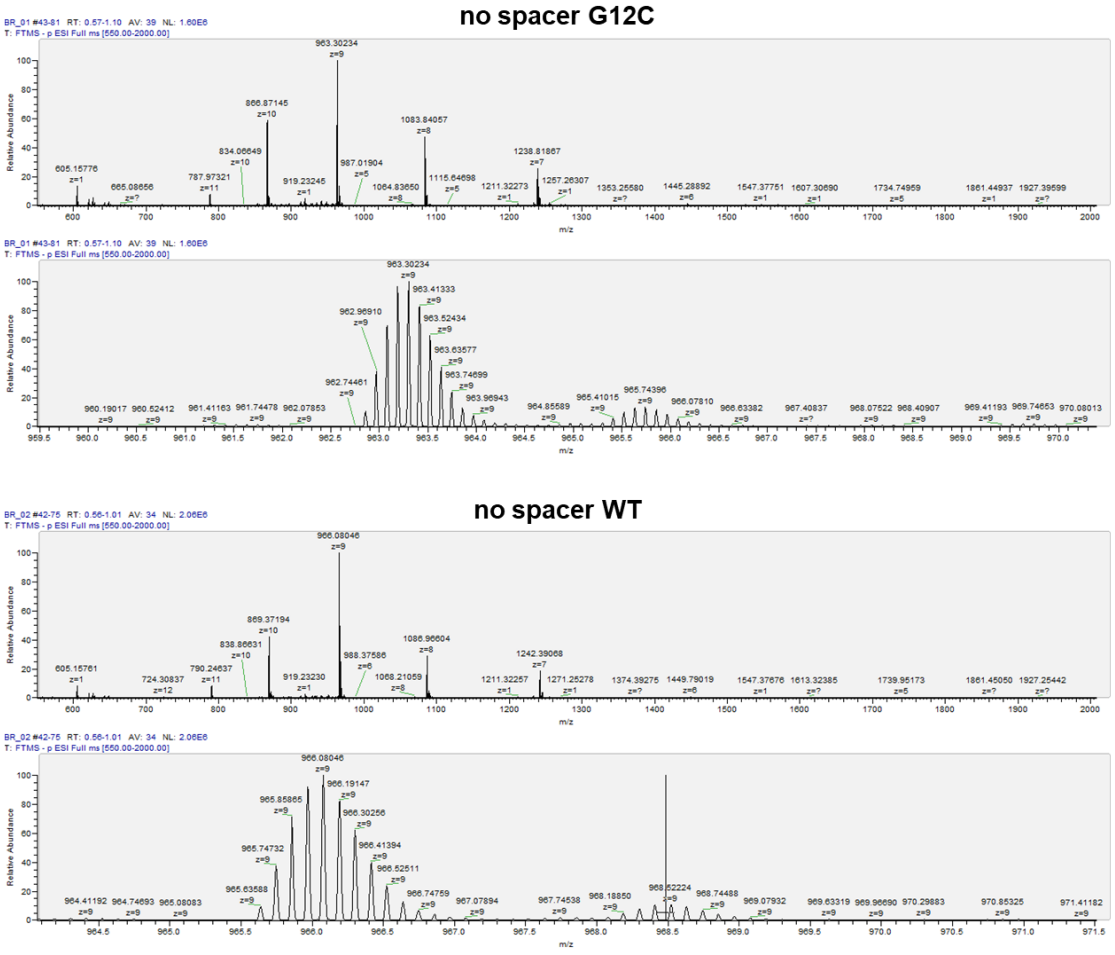

internal short spacer G12C

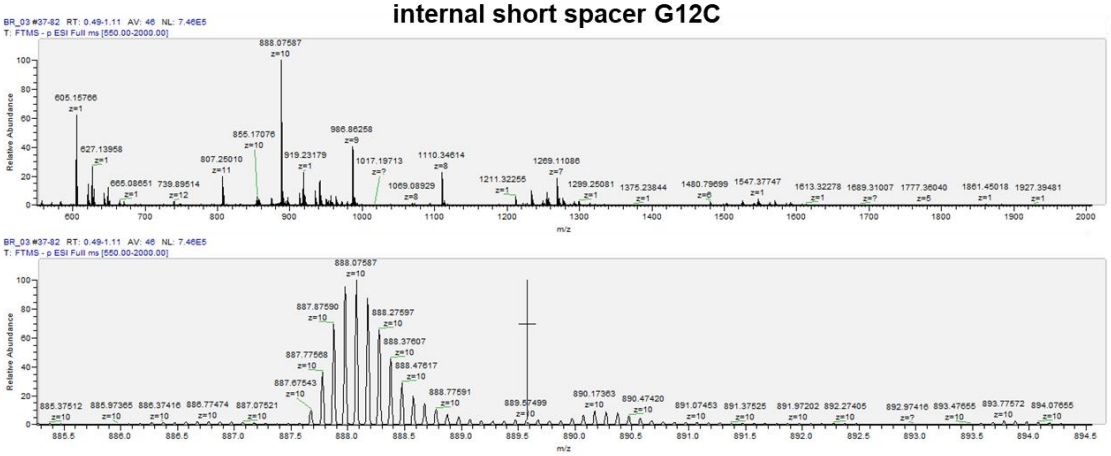

internal short spacer WT

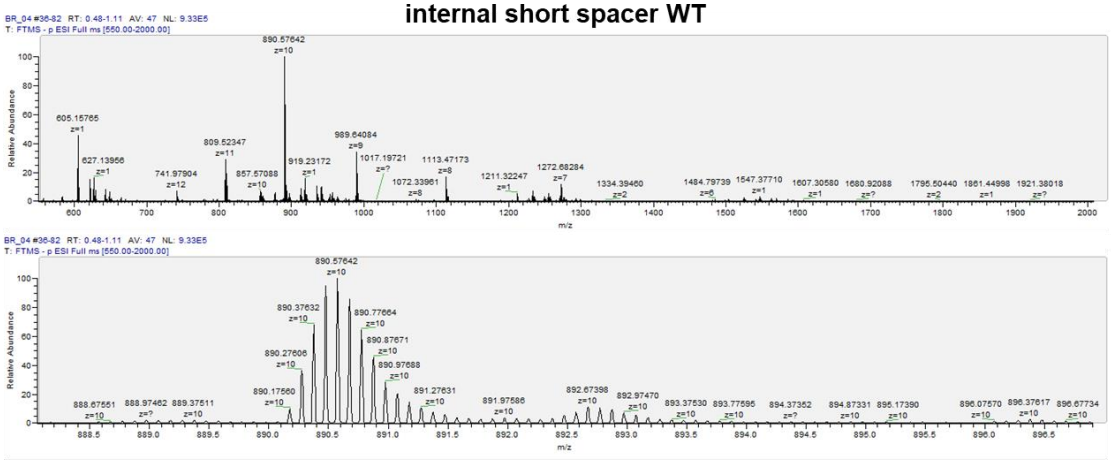

internal long spacer G12C

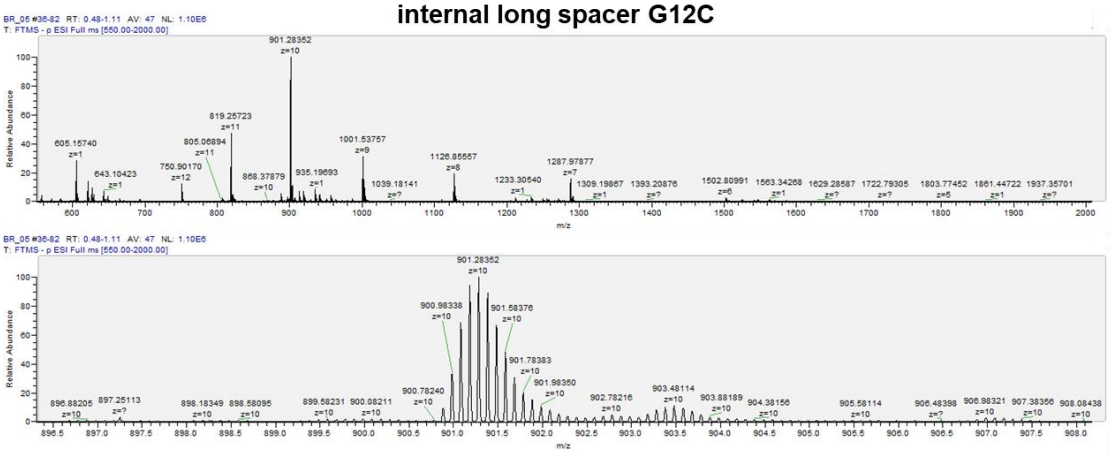

internal long spacer WT

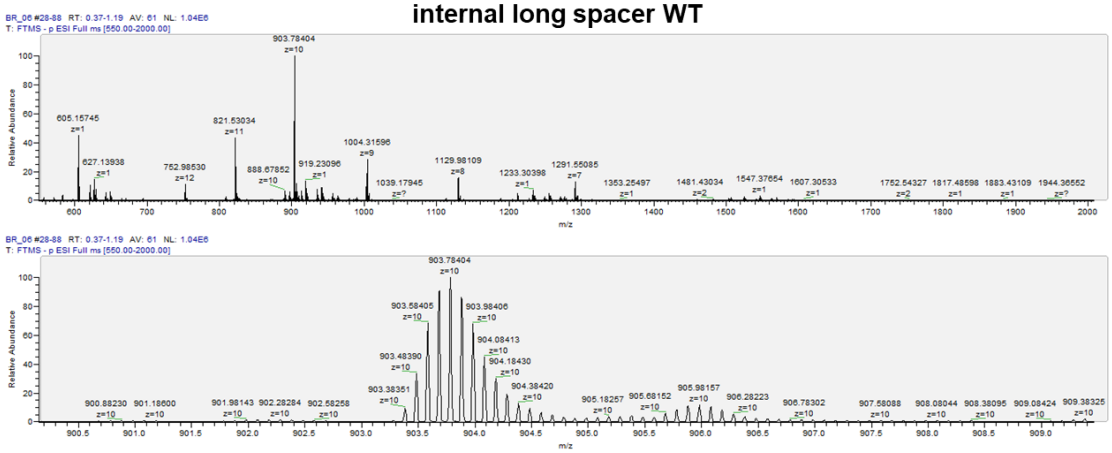

terminal short spacer G12C

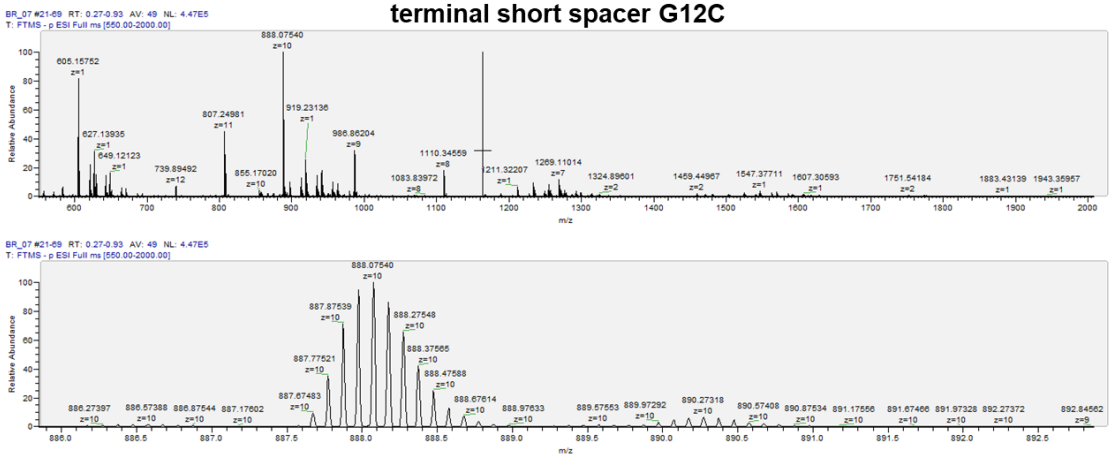

terminal short spacer WT

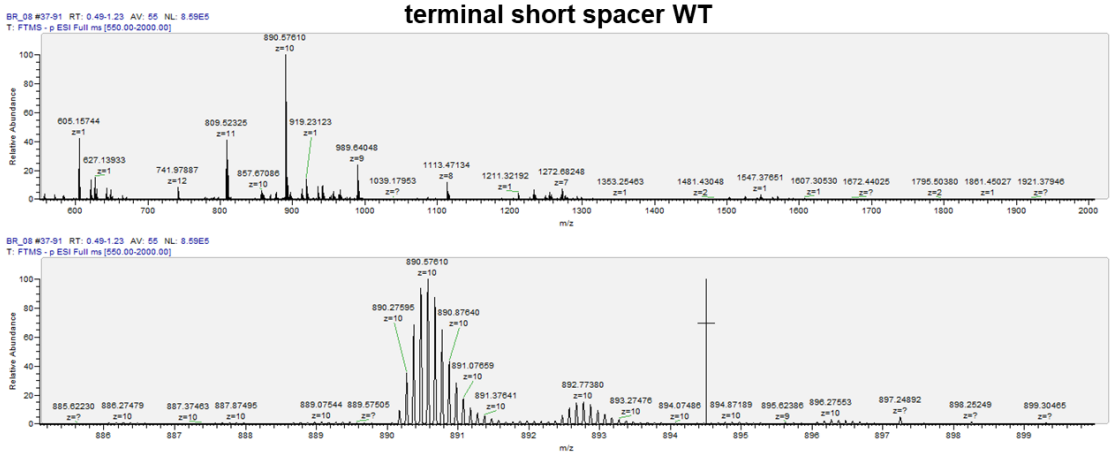

terminal long spacer G12C

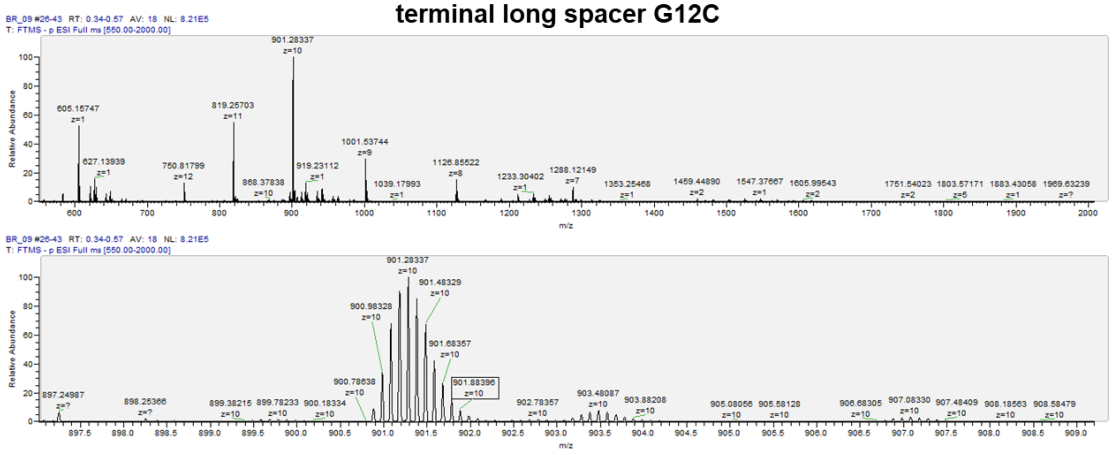

terminal long spacer WT

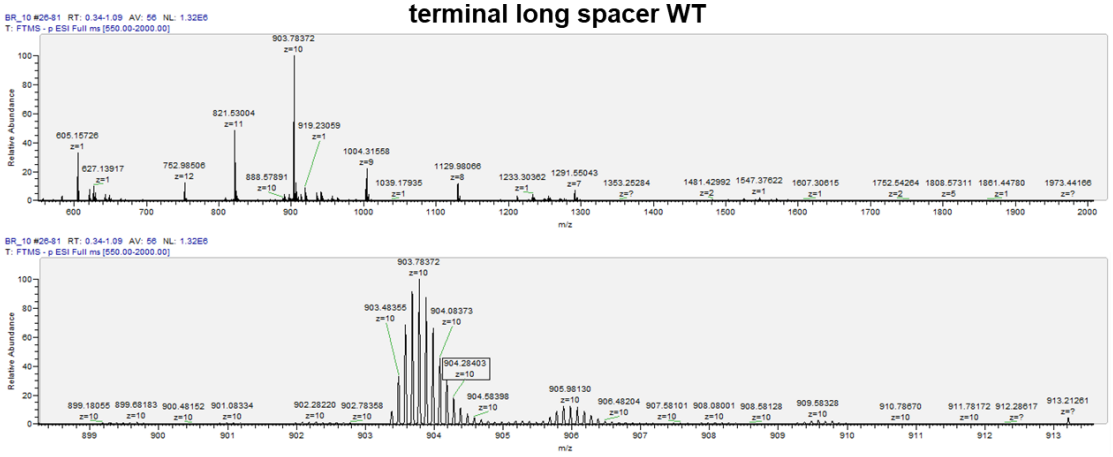

G12C/L19F

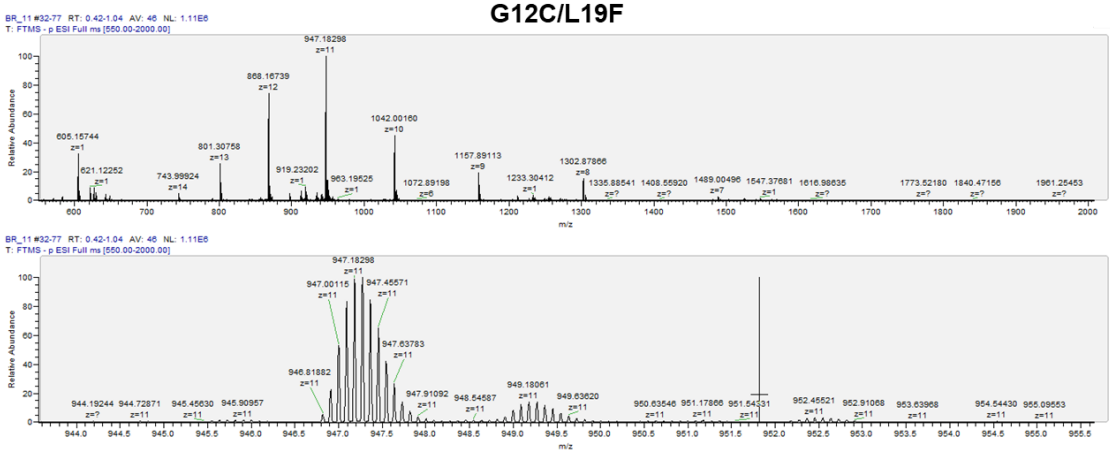

WT/L19F

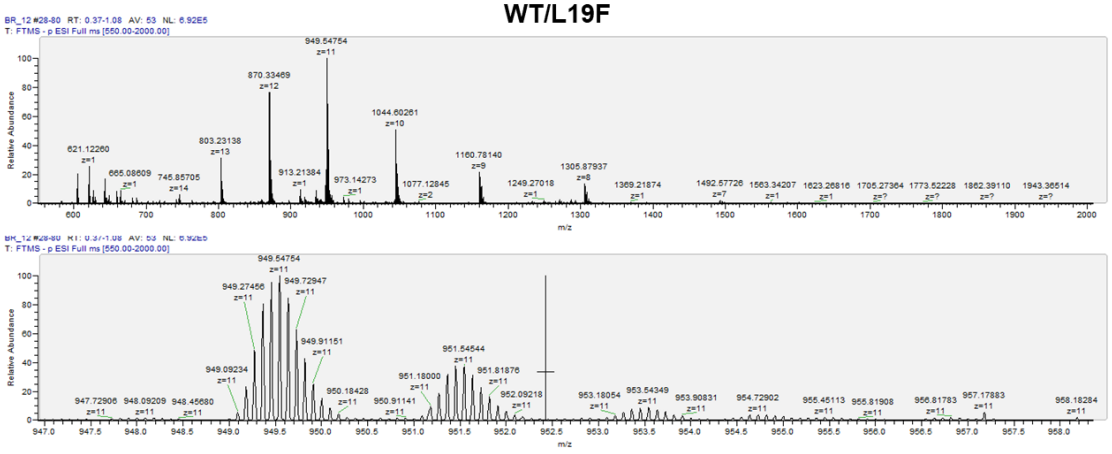

G12C/WT

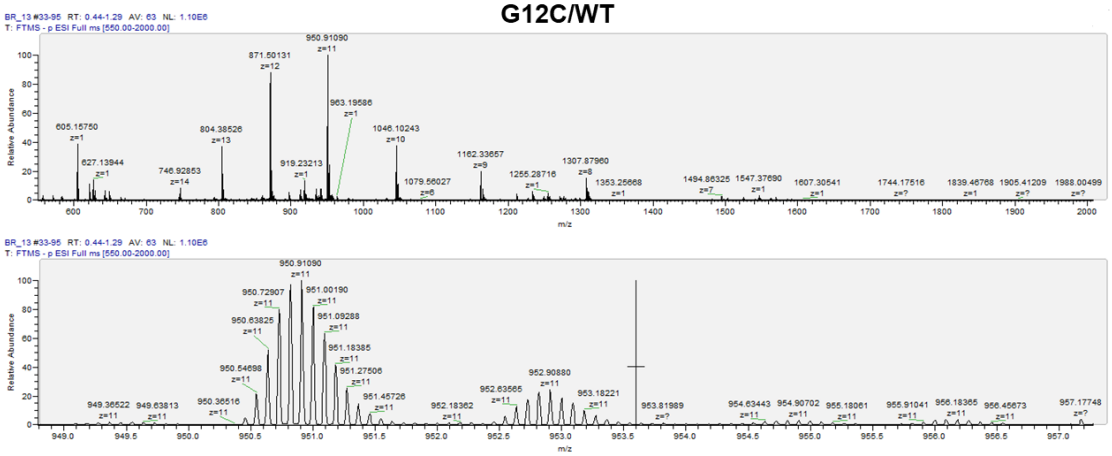

WT/WT

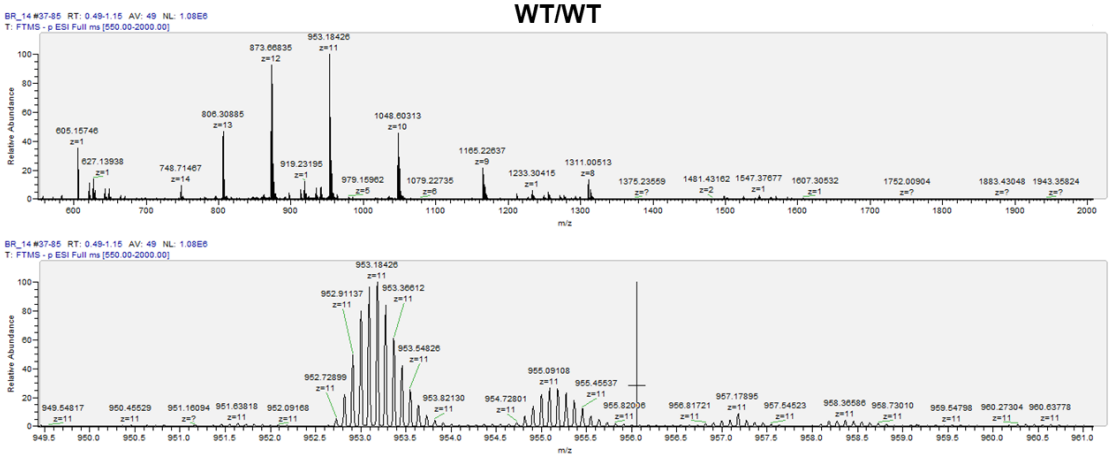

29 nt Original

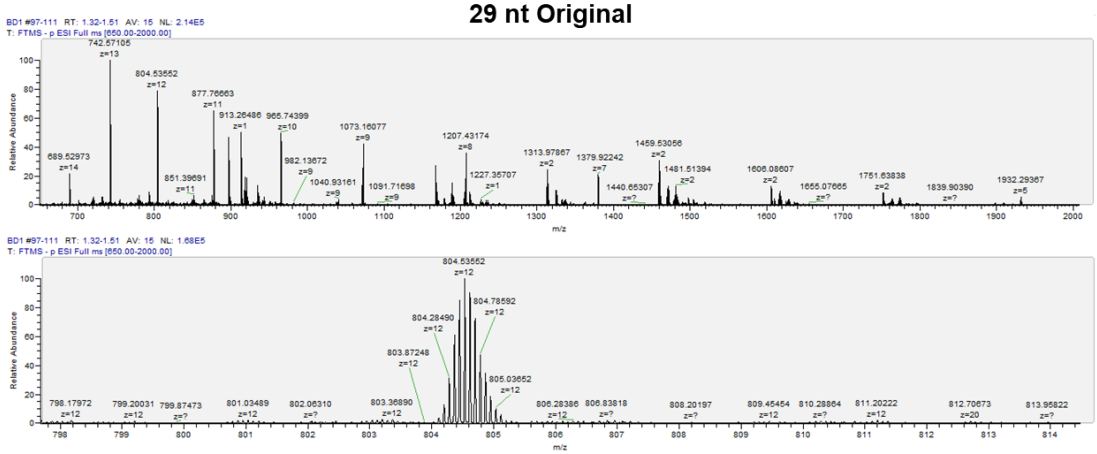

29 nt Alpha

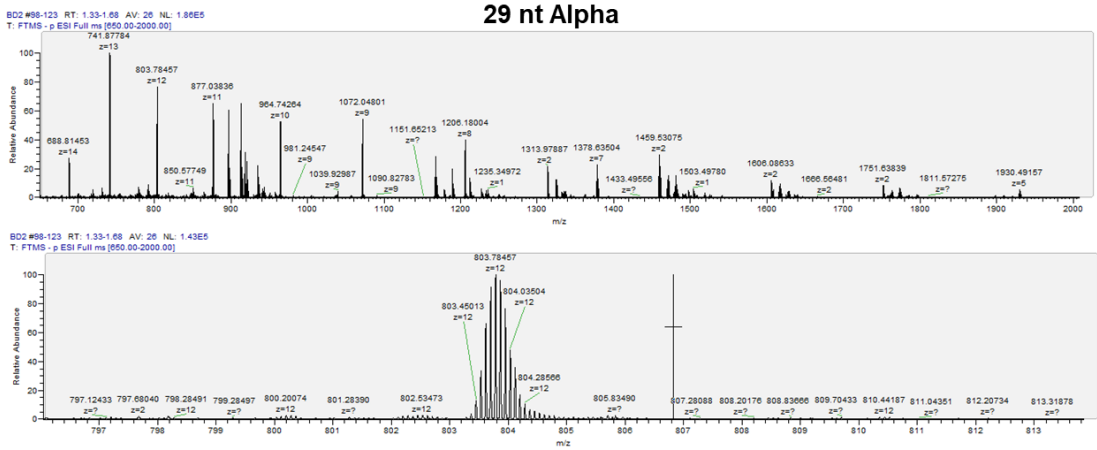

29 nt Omicron

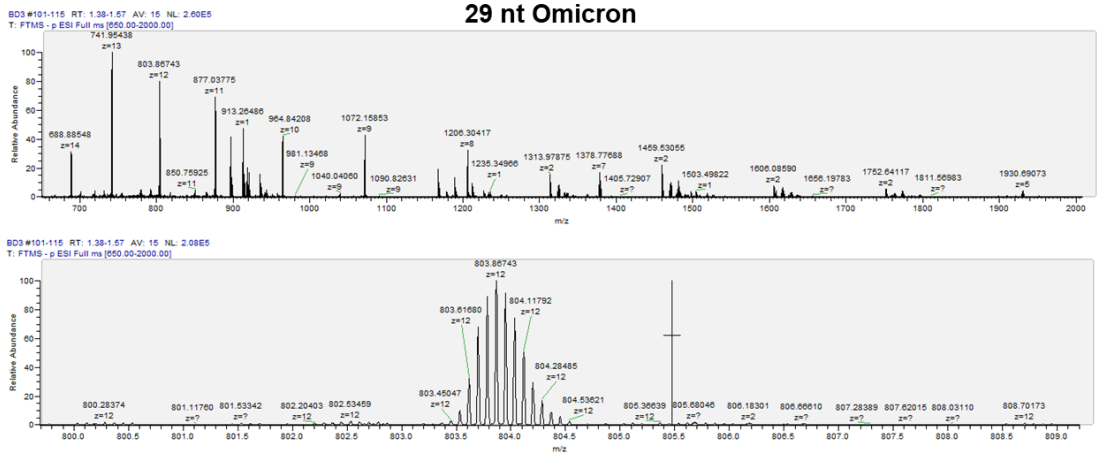

88 nt Original

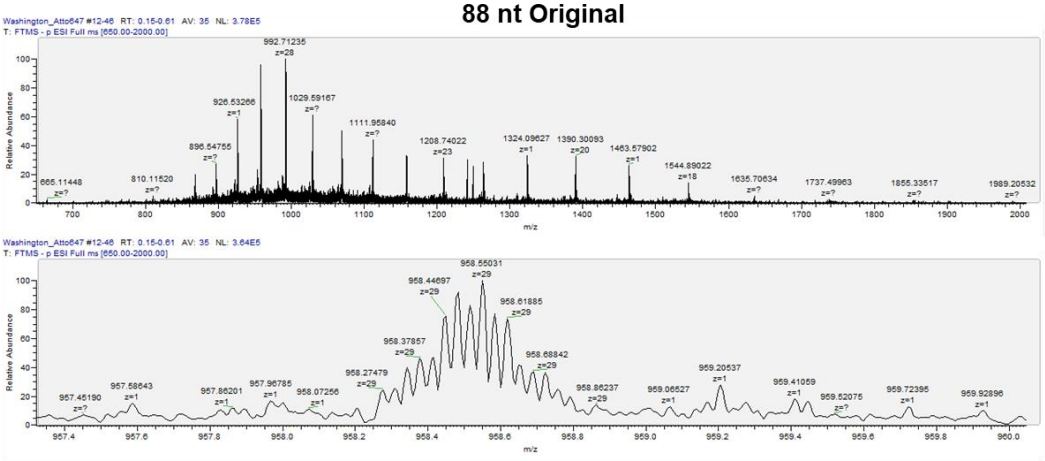

88 nt Omicron

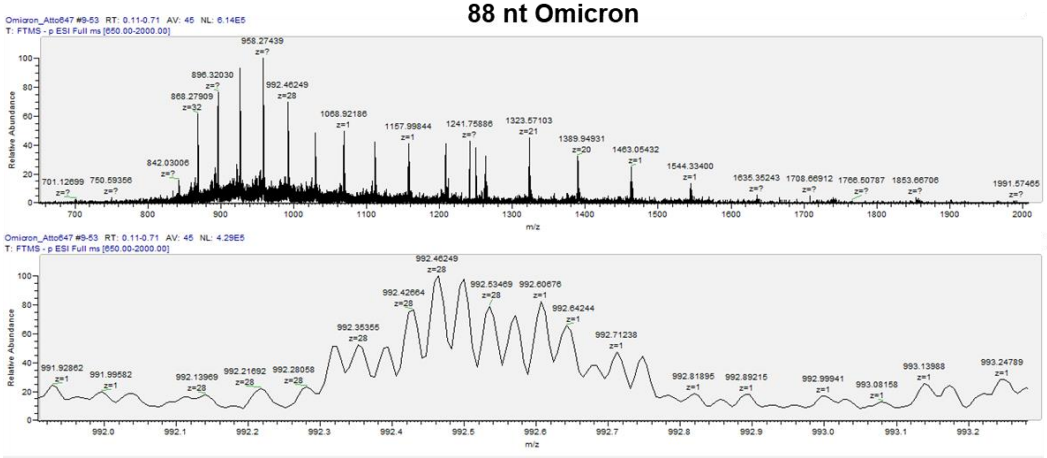

Supplementary Figure 4. Synthesis of DNA-functionalized silica particles.
Scheme describing the synthesis of DNA-functionalized silica particles. On top is a simplified summary of the synthesis, whereas the boxes on the bottom provide further synthetic details and structures of the reagents used. Refer to methods section “Synthesis of DNA-functionalized silica particles” for a complete description of the synthesis.

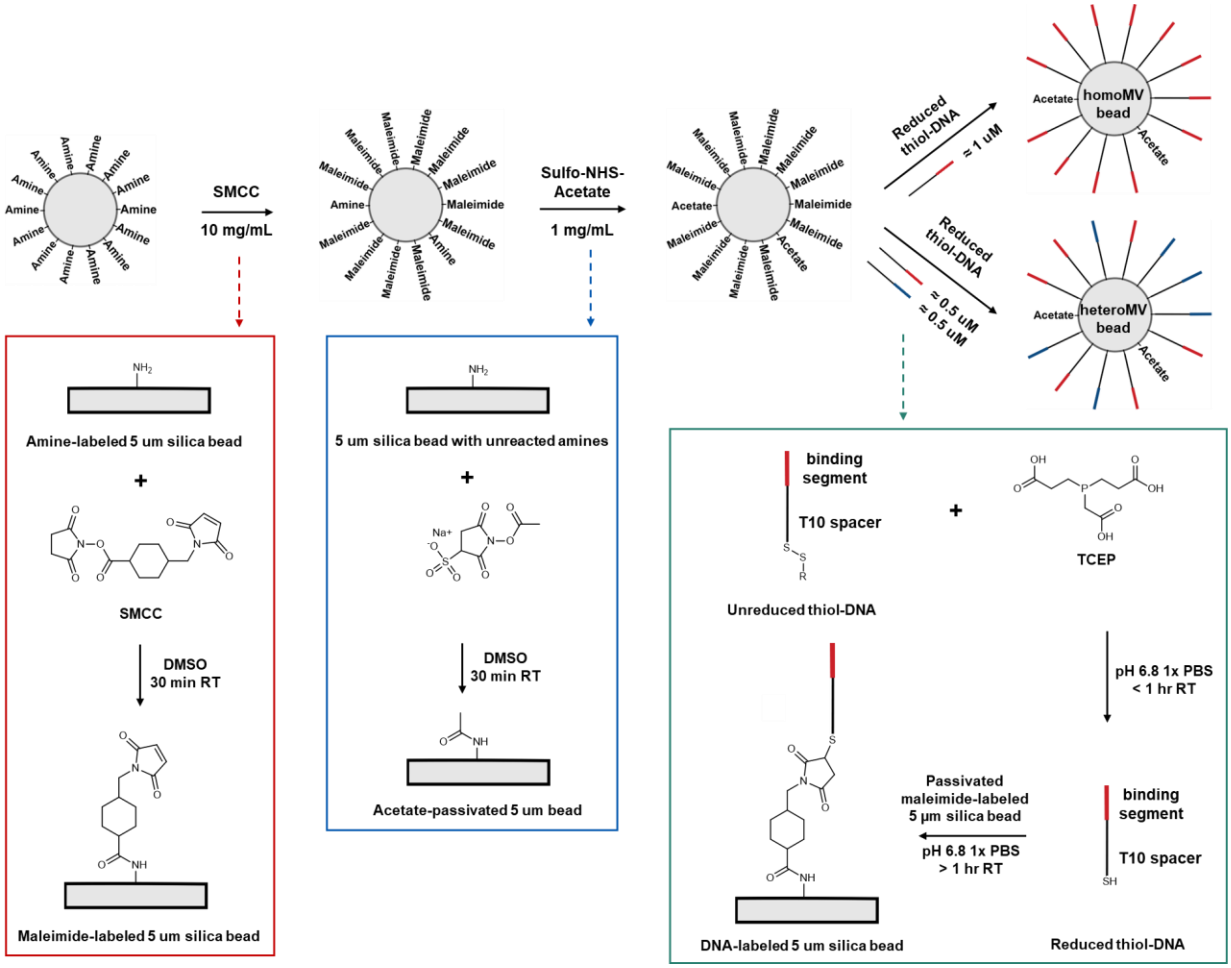

Supplementary Figure 5. Flow cytometry gating strategy to isolate singlet beads for analysis.

(A) For each sample, all events are first plotted on a side scatter area vs forward scatter area plot and a “singlets area” gate is drawn to approximately include just the singlet bead population. (B) The cells included in the “singlets area” gate are then plotted on a side scatter height vs forward scatter height plot and a second gate, the “singlets height” gate, is drawn to more accurately include just the singlet bead population. The cells included in the “singlets height” gate are then used as the final singlet bead population shown in the representative histograms and from which the median fluorescence intensity values were calculated.

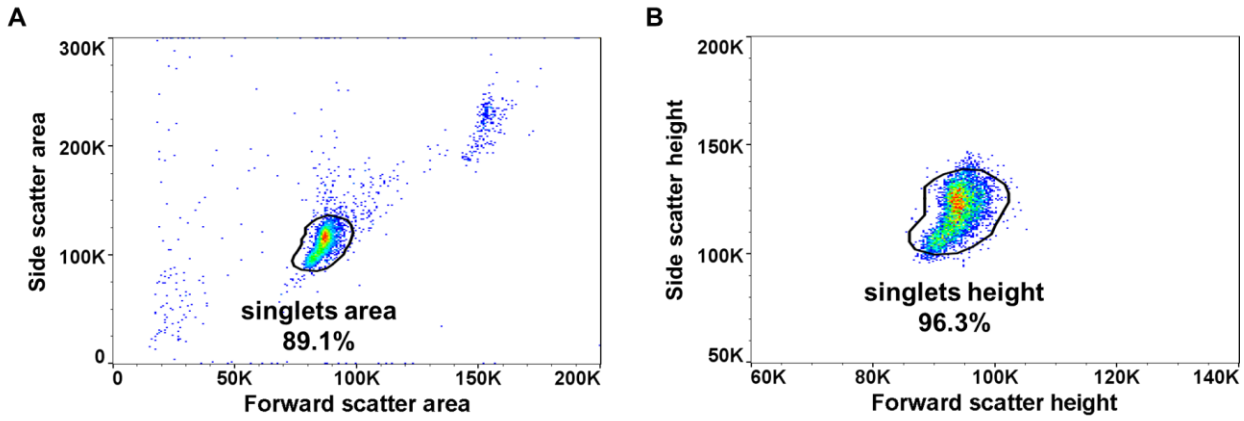

Supplementary Figure 6. Fluorescence microscopy images of beads hybridized to target. Brightfield and epifluorescence microscopy images of full-length complement beads hybridized to 1 nM of Atto647N-labeled Omicron target or no target. Images shown are representative images obtained from a single independent experiment.

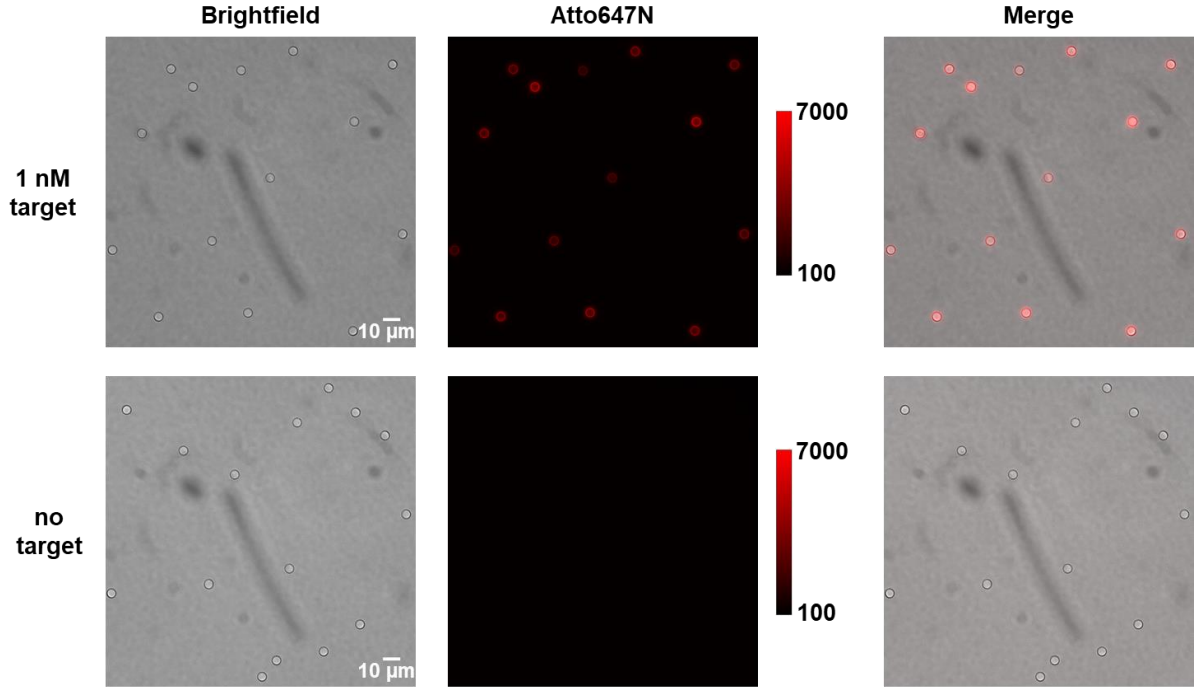

Supplementary Table 1. Average median fluorescence intensity ± standard error of the mean values for all bead combinations binding no spacer G12C target.

The median fluorescence intensity of the no spacer G12C target binding to each bead combination was measured in three independent experiments. The table below shows the calculated average and standard error of the mean for the three median fluorescence intensity values.

	No S	7S	8S	9S	10S	11S
No T	59 ± 4	154 ± 13	517 ± 73	4522 ± 540	15126 ± 1789	35194 ± 935
4T	54 ± 2	120 ± 6	472 ± 33	4939 ± 328	22647 ± 423	34573 ± 1503
5T	93 ± 10	161 ± 26	1076 ± 78	8951 ± 560	14087 ± 589	40989 ± 10285
6T	106 ± 2	298 ± 19	1779 ± 89	15111 ± 396	42858 ± 1714	62873 ± 2816
7T	235 ± 13	424 ± 33	3658 ± 256	20935 ± 2115	51019 ± 5841	68290 ± 1784
8T	2369 ± 118	10610 ± 920	53619 ± 7605	81596 ± 9674	97022 ± 8979	125280 ± 4197
9T	14828 ± 1224	28731 ± 5128	76229 ± 16169	112663 ± 27240	195151 ± 22429	154005 ± 4026
10T	13744 ± 1450	81537 ± 4328	148605 ± 14991	213091 ± 9045	205227 ± 5447	176200 ± 2110

Supplementary Table 2. Average median fluorescence intensity ± standard error of the mean values for all bead combinations binding no spacer WT target.

The median fluorescence intensity of the no spacer WT target binding to each bead combination was measured in three independent experiments. The table below shows the calculated average and standard error of the mean for the three median fluorescence intensity values.

	No S	7S	8S	9S	10S	11S
No T	56 ± 4	64 ± 1	72 ± 3	174 ± 12	661 ± 97	24728 ± 962
4T	61 ± 7	64 ± 3	74 ± 3	213 ± 20	909 ± 72	21385 ± 1218
5T	109 ± 10	75 ± 9	113 ± 4	251 ± 14	1225 ± 78	29084 ± 6095
6T	125 ± 1	118 ± 3	170 ± 5	475 ± 21	4040 ± 346	50386 ± 2148
7T	208 ± 19	139 ± 4	277 ± 11	647 ± 121	7234 ± 404	62561 ± 1675
8T	1955 ± 635	2262 ± 117	2826 ± 58	10898 ± 2346	81904 ± 7503	124810 ± 3137
9T	13597 ± 2110	8693 ± 1292	9635 ± 1436	60413 ± 8188	159425 ± 13751	154441 ± 13439
10T	18205 ± 1140	25845 ± 523	38530 ± 3431	130354 ± 5038	166468 ± 18349	166092 ± 14714

Supplementary Table 3. Average discrimination factor ± standard error of the mean values for all bead combinations binding no spacer targets.

The median fluorescence intensity of the no spacer G12C (**Supplementary Table 1**) and WT (**Supplementary Table 2**) targets binding to each bead combination was measured in three independent experiments. The discrimination factor was calculated for each independent replicate by dividing the G12C MFI value by the WT MFI value. The table below shows the calculated average and standard error of the mean for the three discrimination factor values.

	No S	7S	8S	9S	10S	11S
No T	1.0 ± 0.0	2.4 ± 0.2	7.2 ± 0.8	25.9 ± 1.4	23.2 ± 2.0	1.4 ± 0.1
4T	0.9 ± 0.1	1.9 ± 0.1	6.4 ± 0.3	23.3 ± 0.6	25.2 ± 2.0	1.6 ± 0.0
5T	0.8 ± 0.0	2.1 ± 0.2	9.5 ± 0.7	35.6 ± 1.4	11.5 ± 0.3	1.4 ± 0.1
6T	0.8 ± 0.0	2.5 ± 0.2	10.5 ± 0.8	31.8 ± 0.6	10.7 ± 0.5	1.2 ± 0.0
7T	1.2 ± 0.1	3.1 ± 0.3	13.2 ± 0.6	33.9 ± 4.4	7.1 ± 0.8	1.1 ± 0.0
8T	1.8 ± 1.0	4.7 ± 0.2	18.9 ± 2.3	8.0 ± 1.3	1.2 ± 0.2	1.0 ± 0.0
9T	1.1 ± 0.2	3.3 ± 0.3	7.9 ± 1.1	1.8 ± 0.2	1.2 ± 0.1	1.0 ± 0.1
10T	0.8 ± 0.0	3.2 ± 0.2	3.9 ± 0.6	1.6 ± 0.0	1.3 ± 0.1	1.1 ± 0.1

Supplementary Table 4. Average cooperativity factor ± standard error of the mean values for all bead combinations binding no spacer G12C target.

The median fluorescence intensity of the no spacer G12C (**Supplementary Table 1**) target binding to each bead combination was measured in three independent experiments. The average cooperativity factor was calculated by dividing the average *n*=2 MFI by the average of the average corresponding *n*=1 MFIs. The standard error of the mean was calculated by propagating the SEMs from the three independent MFI measurements for the *n*=2 beads and the *n*=1 beads. The table below shows the calculated average cooperativity factor and standard error of the mean.

	7S	**8S**	**9S**	**10S**	**11S**
4T	1.2 ± 0.1	1.7 ± 0.2	2.2 ± 0.3	3.0 ± 0.4	2.0 ± 0.1
5T	1.3 ± 0.2	3.5 ± 0.5	3.9 ± 0.5	1.9 ± 0.2	2.3 ± 0.6
6T	2.3 ± 0.2	5.7 ± 0.7	6.5 ± 0.8	5.6 ± 0.7	3.6 ± 0.2
7T	2.2 ± 0.2	9.7 ± 1.2	8.8 ± 1.3	6.6 ± 1.1	3.9 ± 0.1
8T	8.4 ± 0.8	37.2 ± 5.6	23.7 ± 3.4	11.1 ± 1.5	6.7 ± 0.3
9T	3.8 ± 0.8	9.9 ± 2.3	11.6 ± 2.9	13.0 ± 1.8	6.2 ± 0.2
10T	11.7 ± 1.4	20.8 ± 3.0	23.3 ± 2.2	14.2 ± 1.2	7.2 ± 0.3